

# Histone Deacetylase Complex1 Expression Level Titrates Plant Growth and Abscisic Acid Sensitivity in *Arabidopsis*<sup>CWJOPEN</sup>

Giorgio Perrella,<sup>a</sup> Manuel A. Lopez-Vernaza,<sup>a,1</sup> Craig Carr,<sup>a</sup> Emanuela Sani,<sup>a,1</sup> Veronique Gosselé,<sup>b</sup> Christoph Verduyn,<sup>b</sup> Fabian Kellermeier,<sup>a</sup> Matthew A. Hannah,<sup>b</sup> and Anna Amtmann<sup>a,2</sup>

<sup>a</sup> Plant Science Group, Institute of Molecular, Cell, and Systems Biology, College of Medical, Veterinary, and Life Sciences, University of Glasgow, Glasgow G128QQ, United Kingdom

<sup>b</sup> Bayer CropScience, B-9052 Ghent, Belgium

**Histone deacetylation regulates gene expression during plant stress responses and is therefore an interesting target for epigenetic manipulation of stress sensitivity in plants. Unfortunately, overexpression of the core enzymes (histone deacetylases [HDACs]) has either been ineffective or has caused pleiotropic morphological abnormalities. In yeast and mammals, HDACs operate within multiprotein complexes. Searching for putative components of plant HDAC complexes, we identified a gene with partial homology to a functionally uncharacterized member of the yeast complex, which we called Histone Deacetylation Complex1 (HDC1). HDC1 is encoded by a single-copy gene in the genomes of model plants and crops and therefore presents an attractive target for biotechnology. Here, we present a functional characterization of HDC1 in *Arabidopsis thaliana*. We show that HDC1 is a ubiquitously expressed nuclear protein that interacts with at least two deacetylases (HDA6 and HDA19), promotes histone deacetylation, and attenuates derepression of genes under water stress. The fast-growing HDC1-overexpressing plants outperformed wild-type plants not only on well-watered soil but also when water supply was reduced. Our findings identify HDC1 as a rate-limiting component of the histone deacetylation machinery and as an attractive tool for increasing germination rate and biomass production of plants.**

## INTRODUCTION

Biochemical modifications of DNA and histones regulate gene expression in eukaryotes at a level that is superimposed onto regulation of promoter activity through transcription factors (Berger, 2007). Modifications of specific histone tail residues, alone and in combination, constitute a histone code that is recognized by the transcriptional machinery. Within this context, deacetylation of Lys residues in histones 3 and 4, catalyzed by histone deacetylases (HDACs), establishes a repressive mark (Kouzarides, 2007; Roudier et al., 2009). In plants, histone deacetylation supports fundamental life functions, including maintenance of genome stability (Probst et al., 2004; To et al., 2011; Liu et al., 2012), determination of cell-type specificity (Xu et al., 2005; Hollender and Liu, 2008), and transition between developmental stages (Tanaka et al., 2008; Yu et al., 2011). Gene repression through histone deacetylation is also an important part of the hormonal signaling pathways that orchestrate plant responses to biotic or abiotic stress factors in the environment (Zhou et al., 2005; Chen et al., 2010; Chen and Wu, 2010). The Class1-

REDUCED POTASSIUM DEPENDENCY3 (Rpd3)-type HISTONE DEACETYLASE6 (HDA6; often acting redundantly with another enzyme of the same family, HDA19) has emerged as a major player in many of these functions (Kim et al., 2012). For example, HDA6 silences transposons and repetitive elements in a process that is at least partially coupled to DNA methylation (Probst et al., 2004; To et al., 2011; Liu et al., 2012). HDA6 and HDA19 redundantly silence embryonic genes after germination, and in mature plants, HDA6 induces flowering by repressing the flowering inhibitor FLOWERING LOCUS C (FLC; Tanaka et al., 2008; Yu et al., 2011). Furthermore, HDA6 and HDA19 are required for jasmonate/ethylene-mediated defense responses to pathogens (Zhou et al., 2005; Zhu et al., 2011) and for abscisic acid (ABA)-mediated responses to drought or salt (Chen et al., 2010; Chen and Wu, 2010).

Current mechanistic models of how histone deacetylation modulates gene transcription are primarily based on work performed in yeast and mammalian cells showing that de novo nucleosome assembly, chromatin compaction, and recruitment of transcriptional repressors all depend on the acetylation status of histone proteins, which affects the electrostatic histone–DNA interaction and higher-order folding of the chromatin (Kurdistani and Grunstein, 2003; Shahbazian and Grunstein, 2007). Histone deacetylation can occur globally, affecting contiguous regions of the euchromatin, or locally, after recruitment of HDACs by site-specific DNA binding proteins. To enable these processes, HDACs interact with other proteins that establish a structural link between the core deacetylation enzymes, the histones, and the DNA. Several such multiprotein complexes have been biochemically purified in yeast and mammalian cells (Carrozza et al., 2005a, 2005b; Roguev and Krogan, 2007; Yang and Seto, 2008; Chen et al., 2012).

<sup>1</sup> Current address: Institute of Cell Biology, University of Edinburgh, Edinburgh EH9 3JR, United Kingdom.

<sup>2</sup> Address correspondence to anna.amtmann@glasgow.ac.uk. The author responsible for distribution of materials integral to the findings presented in this article in accordance with the policy described in the Instructions for Authors (www.plantcell.org) is: Anna Amtmann (anna.amtmann@glasgow.ac.uk).

Some figures in this article are displayed in color online but in black and white in the print edition.

Online version contains Web-only data.

Articles can be viewed online without a subscription.

www.plantcell.org/cgi/doi/10.1105/tpc.113.114835

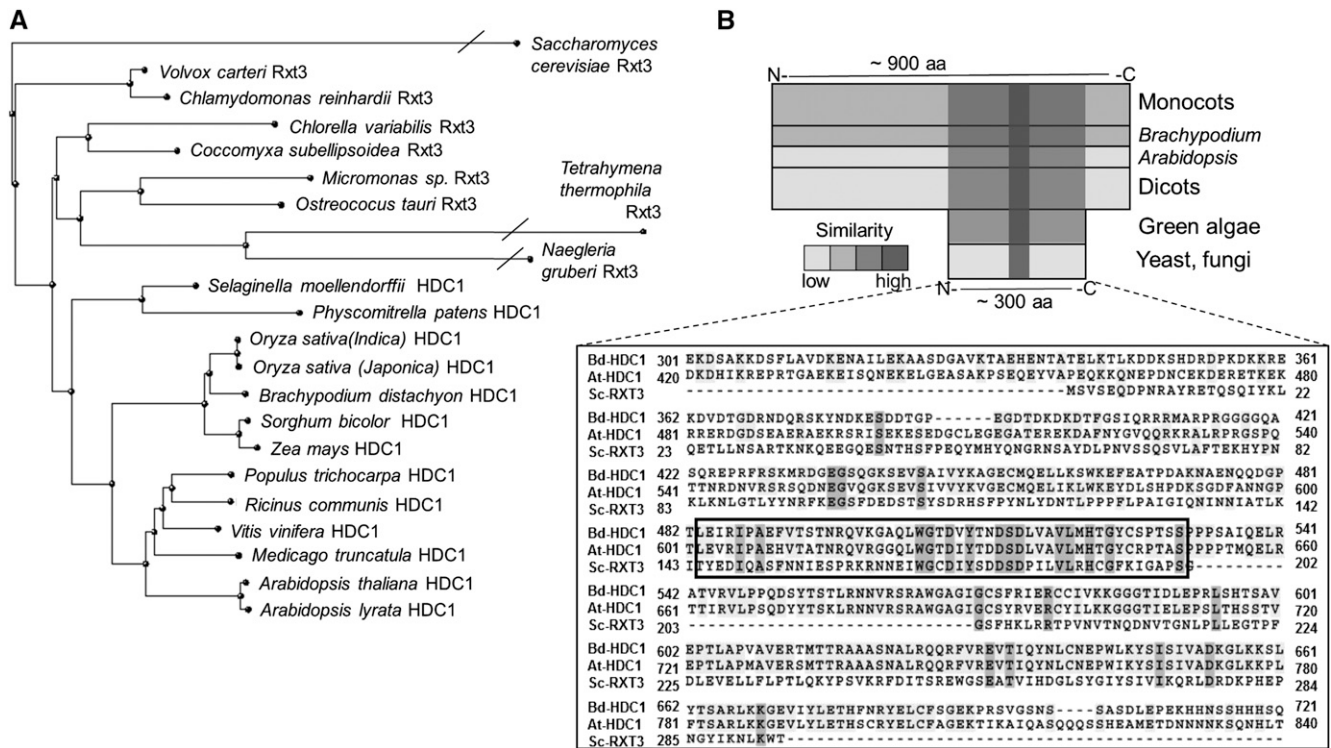


**Figure 1.** Plant HDC1 Proteins Have Extended from Ancestral Rxt3 Proteins in Fungi and Algae.

**(A)** Cluster dendrogram of predicted protein sequences of *HDC1/Rxt3* genes in yeast, algae, protozoa, mosses, and land plants, underlying the sequence alignment provided in Supplemental Data Set 1 online.

**(B)** Schematic view of conserved and novel parts of plant HDC1 proteins. For the Rxt3 part of the protein, an alignment of the *Arabidopsis* (At) sequence with sequences from *Brachypodium distachyon* (Bd) HDC1 and yeast (Sc) Rxt3 is inserted. Identical amino acids are highlighted in gray. A conserved protein domain family signature histone deacetylation Rxt3 (PF08642) is marked with a box. aa, amino acids.

Each of them comprises a distinct set of proteins. For example, so-called Sin3 complexes contain a core deacetylase (Rpd3 and HDAC1/2), a corepressor protein (SWI-INDEPENDENT3 [SIN3]), SIN3-associated proteins, histone binding proteins, and DNA binding proteins. Plant HDAC complexes have not yet been biochemically purified, but several genes with homology to the above-listed HDAC-interacting proteins have been functionally characterized in *Arabidopsis thaliana*, including *SIN3* (Song et al., 2005) and *SAP18* (Song and Galbraith, 2006), as well as histone binding proteins *MULTICOPY SUPPRESSOR OF IRA1 4/5* (Gu et al., 2011) and *HIGH EXPRESSION OF OSMOTICALLY RESPONSIVE GENES15* (Zhu et al., 2008). Protein interaction assays and mutant analysis firmly placed these proteins into HDA6/19-regulated pathways, thus providing strong evidence that plant HDACs, as their counterparts in other eukaryotes, operate within multiprotein complexes.

HDACs provide interesting targets for epigenetically engineering stress responses in plants, bypassing the requirement to manipulate many individual components of a complex signaling network. However, the fact that they operate within multiprotein complexes represents a problem for achieving quantitative effects. Indeed, no phenotypes have been reported for overexpression of HDA6. Furthermore, a high degree of redundancy can be expected because HDACs and interacting proteins are encoded by large gene families, suggesting that different

complexes assemble depending on tissue type, developmental stage, and environmental condition.

With the aim to identify potential candidate genes for epigenetic manipulation of stress sensitivity in plants, we performed a comprehensive search for plant homologs of confirmed components of yeast and mammalian histone deacetylation complexes. We identified one gene that occurred as a single-copy gene in all sequenced plant genomes, which we called Histone Deacetylation Complex1 (HDC1). HDC1 has partial homology to Regulator of transcription3 (Rxt3), a 34-kD protein of unknown function that coelutes with the large Rpd3 complex in yeast (Carozza et al., 2005b). However, the function of *HDC1* cannot be inferred without further analysis. The functions of *Rxt3*-type and *HDC1*-type genes have not been clarified, and neither of them contains any known functional motifs. Furthermore, the plant genes are considerably longer than the ancestral *Rxt3* genes and could have acquired new functions.

Here, we present a functional characterization of *HDC1* in *Arabidopsis*. We show that HDC1 interacts with HDACs, promotes histone deacetylation, and regulates known downstream processes, such as ABA sensitivity and flowering. Furthermore, we found that HDC1 overexpression increases plant biomass production. Our results identify HDC1 as a nonredundant, ubiquitous, rate-limiting component of the histone deacetylation

machinery, which offers opportunities for improving plant performance with limited water supply.

## RESULTS

### HDC1 Is a Nonredundant, Ubiquitous, Nuclear Protein

*HDC1* (At5g08450) is a single-copy gene in *Arabidopsis*. Predicted splice variants only differ in the upstream untranslated region. Unique *HDC1* homologs are also present in all other plant species for which genome information is currently available, including important crops, such as maize (*Zea mays*) and rice (*Oryza sativa*; Figure 1A). The ~900-amino-acid-long sequence of the predicted plant HDC1 proteins contains an ~300-amino-acid-long sequence in the C-terminal half that is highly similar to Rxt3 proteins, which are ubiquitously present in fungi, algae, and protozoa but remain functionally uncharacterized (Figure 1B). Particularly high sequence similarity occurs in a Protein domain family signature (PF08642) labeled as “histone deacetylation Rxt3” (box in Figure 1B). The term derives from biochemical evidence that yeast Rxt3 coelutes with the large Rpd3 complex (Carrozza et al., 2005b), but the region has no homology to catalytic domains of HDACs. Based on sequence similarity, no obvious function can be assigned to this or any other part of the HDC1 sequence. The more variable extended N-terminal part of HDC1 has no counterpart in non-plant genomes. Sequence extension from Rxt3 to HDC1 occurred between algae and land plants, with mosses showing intermediate length (see sequence alignment in Supplemental Data Set 1 online).

The notion of a conserved nonredundant function of HDC1 is supported by ubiquitous expression within the plant. Histochemical analysis of stable *Arabidopsis* lines expressing  $\beta$ -glucuronidase (GUS) under the control of the *HDC1* promoter revealed *HDC1* promoter activity in all vegetative tissues, including seed, root, cotyledon, rosette leaf, and flower bud (Figures 2A to 2E). However, GUS was not detected inside anthers and stigmas (Figures 2F), indicating that *HDC1* is silenced during reproduction. This is in accordance with a general resetting of chromatin status during reproduction (Paszowski and Grossniklaus, 2011).

Visualization of a green fluorescent protein (GFP)–HDC1 fusion protein in transiently expressing tobacco (*Nicotiana tabacum*) plants and in stable transgenic *Arabidopsis* plants showed exclusive presence of HDC1 in the nucleus (Figures 2G and 2H) but not in the nucleolus (Figure 2I).

### HDC1 Physically Interacts with HDA6 and HDA19 and Promotes Histone Deacetylation

To investigate whether HDC1 is a member of HDAC protein complexes in plants, we tested colocalization and direct interaction of HDC1 with known HDACs of *Arabidopsis*. Coexpression of full-length GFP–HDC1 with red fluorescent protein (RFP)–HDA6 or RFP–HDA19 in epidermal tobacco cells indicated tight colocalization of HDC1 with HDA6 and HDA19 in different locations within the nucleus (see Supplemental Figure 1 online). Direct interaction was investigated by bimolecular fluorescence complementation (BiFC). To avoid misinterpretation of background fluorescence, we used a new ratiometric BiFC assay (Grefen and Blatt, 2012) in which N- and C-terminal halves of

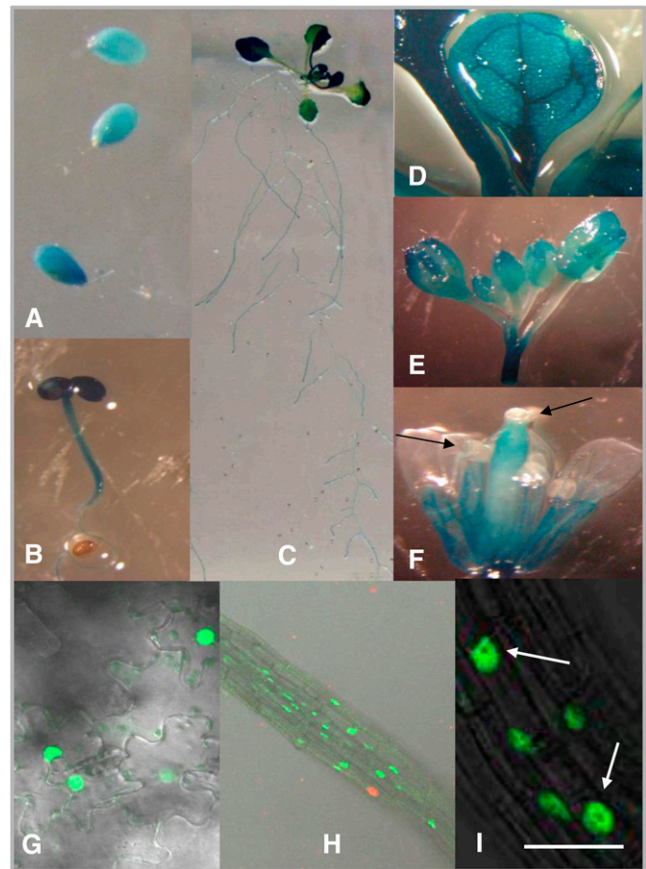


**Figure 2.** HDC1 Is a Ubiquitous Nuclear Protein.

Tissue expression pattern and subcellular localization of HDC1. GUS staining shows *HDC1* promoter activity in seeds (A), root and shoot of seedlings (B) and mature plants (C), rosette leaves (D), and flower buds (E). No staining is visible inside anthers or stigmas (F, arrows). Nuclear localization of GFP–HDC1 in epidermal leaf cells of transiently expressing *N. tabacum* (G) and in root cells of stably expressing *Arabidopsis* plants (H) and (I). No GFP signal is seen inside the nucleolus (I, arrows). Bar in (I) = 50  $\mu$ m.

yellow fluorescent protein (YFP), fused to HDC1 and HDA6/19, respectively, and a full-length RFP are expressed from a single vector (Figure 3A). In RFP-producing cells, a strong YFP signal was recorded for HDA6 and for HDA19, indicating successful BiFC and, hence, interaction of HDC1 with both HDACs. BiFC was also successful when HDA19 was coexpressed with SIN3 previously shown to interact with HDA19 in yeast two-hybrid assays (Song et al., 2005). By contrast, no YFP signal was recorded for HDC1 and SIN3, indicating that HDC1 does not interact with all HDAC complex proteins. Normalization of the obtained YFP signal to the RFP signal from the same cell (Figure 3B) provided statistically significant, quantitative evidence for a strong and specific interaction of HDC1 with the two deacetylases in the heterologous system (Figure 3C).

In vitro pull-down experiments using glutathione S-transferase (GST)- and His-tagged recombinant proteins further confirmed

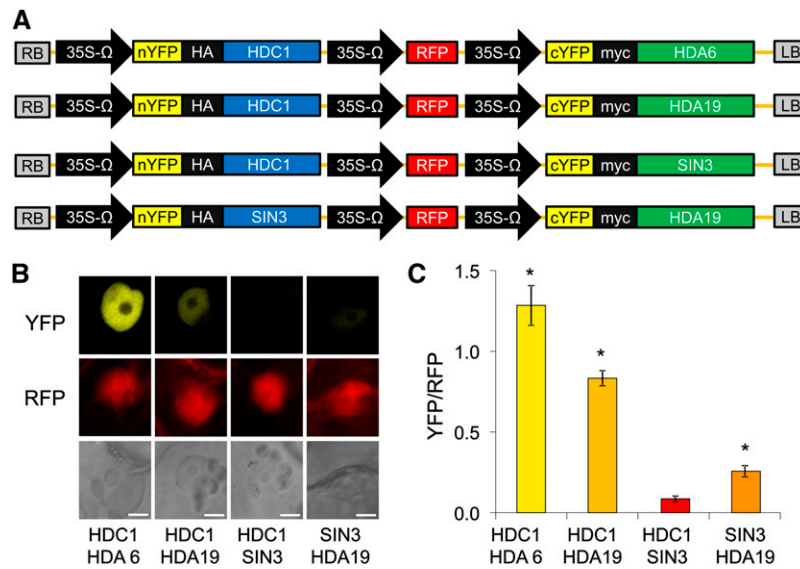


**Figure 3.** HDC1 Interacts with HDACs HDA6 and HDA19 in a Ratiometric BiFC Assay.

**(A)** Two-in-one vectors constructed for ratiometric BiFC assay containing N- and C-terminal halves of YFP (nYFP and cYFP) fused to HDC1, HDA6, HDA19, and SIN3 as well as a full-length RFP.

**(B)** Signals of YFP (top row) and RFP (middle row) in nuclei of tobacco leaf cells after transient expression of nYFP-HDC1 with cYFP-HDA6, cYFP-HDA19, or cYFP-SIN3 (negative control). nYFP-SIN3 was also expressed with cYFP-HDA19 (positive control). The bottom row shows the bright-field image. Bar = 10  $\mu$ m.

**(C)** YFP/RFP signal ratio in individual nuclei (means  $\pm$  SE,  $n \geq 20$  cells from three independently transformed plants). Asterisks indicate significant differences ( $P < 0.001$ ) to the signal ratio obtained for HDC1-SIN3.

the ability of HDC1 to physically interact with HDA6 and HDA19 (Figure 4A). Using GST-HDA6 or GST-HDA19 as bait, HDC1 was pulled down in nuclei-enriched protein samples obtained from leaves of mature *Arabidopsis* plants (Figure 4B). A single band for HDC1 was detected in these assays, indicating that additional modified or truncated forms of HDC1 in the *in vitro* system (triple band in Figure 4A) were not produced in planta. HDC1 was not recovered in pull-down assays with GST alone. No HDC1 was detected when the same assays were performed with protein extract from a T-DNA insertion knockout line, *hdc1-1* (for mutant description, see below).

To test whether HDC1 had an influence on histone deacetylation activity in the plant, we probed leaf protein extracts from wild-type and mutant lines with a commercial antibody that recognizes acetylated Lys residues 9 and 14 in histone 3 (anti-H3K9K14ac), a predominant target of HDA6 (To et al., 2011). As shown in Figure 4C, *hdc1-1* knockout plants produced a significantly higher H3K9K14ac:H3 signal ratio than wild-type plants, indicating higher levels of the acetylated form of H3 over the deacetylated form. Expression of the genomic sequence of HDC1 under its own promoter in the *hdc1-1* background (*HDC1c*) reverted this phenotype; H3K9K14ac:H3 in the complementation line was similar to the wild type (Figure 4C). We conclude that HDC1 interacts with HDACs and is required for HDAC activity in planta.

#### Mutant Lines for Functional Characterization of HDC1

To investigate physiological functions of HDC1, we generated several homozygous lines from currently available *Arabidopsis*

lines with T-DNA insertions in HDC1 coding sequence or untranslated regions (Salk 043645, Salk150126C, SAIL1263E05, and GABI-Kat054G03, all in Columbia-0 [Col-0] background). Only one of these, *hdc1-1*, derived from GABI-Kat, with a T-DNA insertion in the first intron, proved to be a true knockout of HDC1 at the transcript and protein level (see Supplemental Figures 2A to 2C online). *HDC1* transcript levels in the other T-DNA insertion lines were similar to those in the wild type or even higher (see Supplemental Figures 3A and 3B online). Some partial mRNA but no HDC1 protein (full-length or partial) was detected in *hdc1-1* plants (see Supplemental Figure 2C online). *HDC1c* complementation lines were obtained by expressing genomic *HDC1* under its own promoter (646-bp upstream sequence) in *hdc1-1* background. We also produced stable homozygous *HDC1*-overexpressing lines in Col-0 background using either 35S or Ubiquitin-10 promoter (*HDC1-OX1* and *HDC1-OX2*, respectively). Both lines produced  $\sim 30$ -fold higher *HDC1* mRNA levels than the Col-0 wild type (see Supplemental Figure 2D online).

#### HDC1 Determines the Set Point of ABA Sensitivity during Germination

It was previously reported that *hda6* and *hda19* mutant lines are hypersensitive to ABA during germination (Chen et al., 2010; Chen and Wu, 2010). Germinating seeds arrest growth and development if they encounter low water potentials in the environment (Finkelstein et al., 2008). The postimbibition response is mediated by ABA and can be mimicked by external application of

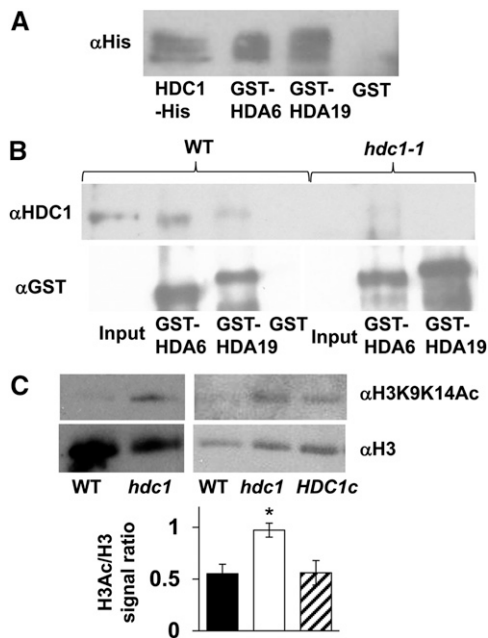


**Figure 4.** HDC1 Interacts with HDACs in Planta and Facilitates H3K9/14 Deacetylation.

**(A)** Anti-His protein gel blots of recombinant HDC1-His after in vitro pull-down with recombinant GST-HDA6 (second lane) and GST-HDA19 (third lane). The first lane contains a positive control (recombinant HDC1-His), and the last lane contains a negative control (pull down with GST alone).

**(B)** Anti-HDC1 protein gel blots of native HDC1 after pull-down from nuclei-enriched protein samples of wild-type (WT, left) or HDC1 knockout plants (*hdc1-1*, right) with recombinant GST-HDA6 (second lanes) or GST-HDA19 (third lanes). HDC1 is recognized in the untreated protein samples from the wild type (input) and in wild-type samples after pull-down with GST-HDA6/19 but not with GST alone. HDC1 is not found in protein samples (input or pull-downs) from knockout plants. The bottom panel shows the membrane re-probed with anti-GST, confirming presence of the bait.

**(C)** Protein gel blot with anti-H3K9K14ac shows increased amounts of acetylated H3K9K14 in protein extract from *hdc1-1* plants compared with the wild type (left blot). After complementation of *hdc1-1* with *HDC1* (*HDC1c*), H3K9K14ac is reverted to the wild-type level (right blot). Total H3 (loading control) was detected with anti( $\alpha$ )-H3. H3K9K14Ac/H3 signal ratios in wild-type, *hdc1-1*, and *HDC1c* lines were determined after quantification of bands with Image J. Bars are means  $\pm$  SE from at least three protein gel blots. Asterisk indicates significant ( $P < 0.05$ ) difference to the wild type and *HDC1c*.

ABA. Gibberellin (GA) antagonizes ABA in this response and, hence, seedling growth arrest also occurs if the GA biosynthesis inhibitor paclobutrazol (PAC) is applied (Daszkowska-Golec, 2011). To test a function of HDC1 in this process, seeds of *Arabidopsis* wild-type, *hdc1-1*, and *HDC1-OX* lines were imbibed to break dormancy and subsequently plated out on agar plates containing different concentrations of sodium chloride (NaCl), mannitol, ABA, or PAC. A cumulative germination rate (encompassing all postimbibition stages of seedling development) was scored as the number of seedlings that had developed cotyledons

after 6 d. In control conditions, all lines germinated similarly well (close to 100%), and germinated seedlings were similar in size and shape (Figure 5; see Supplemental Figure 4A online). All lines showed a decrease in germination rates with increasing concentrations of NaCl, mannitol, ABA, or PAC; however, compared with the wild type, *hdc1-1* was significantly more sensitive, whereas the *OX* lines were significantly less sensitive to the treatments. Hyposensitivity was observed in both *OX* lines, independent of promoter or insertion site. Homozygous lines derived from Salk150126C and SAIL1263E05 displayed similar or slightly decreased ABA sensitivity during germination in accordance with a moderate increase of HDC1 mRNA in these lines (see Supplemental Figure 3C online). We conclude that the expression level of HDC1 quantitatively determines the set point of ABA sensitivity in germinating seeds.

The fact that HDC1 overexpression had a desensitizing effect on ABA-dependent germination was interesting because *HDA6* overexpression had not been proven to produce physiological phenotypes. We therefore assessed ABA sensitivity in seedlings of an *HDA6*-overexpressing line previously generated for biochemical studies (Gu et al., 2011). *35S:HDA6* seedlings showed similar ABA sensitivity as wild-type plants, and they were considerably more sensitive to ABA than *HDC1-OX* seedlings despite a similar increase in transcript level (see Supplemental Figures 5A and 5B online).

To test whether histone deacetylation was required for ABA dependence of seed germination and for the effect of HDC1 on

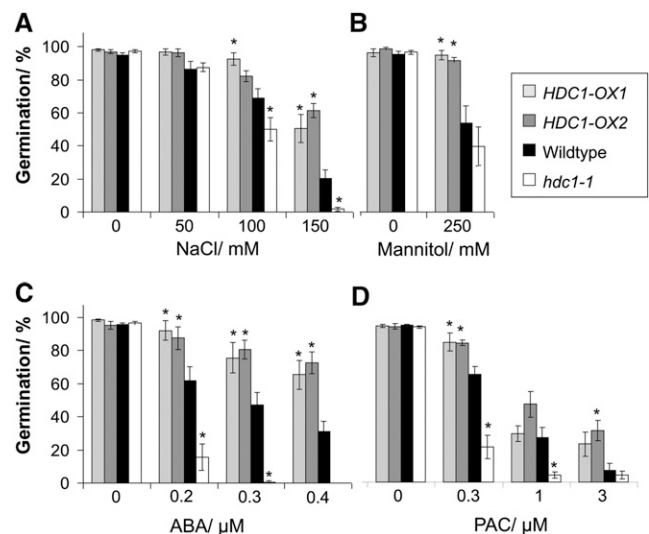


**Figure 5.** HDC1 Desensitizes Seedlings to Salt, Mannitol, ABA, and PAC.

Germination rates of *Arabidopsis* wild-type (black), *hdc1-1* knockout (white), and *HDC1*-overexpressing (*OX*) lines (gray) on agar containing different concentrations of salt (NaCl; **A**), mannitol (**B**), ABA (**C**), or GA biosynthesis inhibitor PAC (**D**). Germination rates in percentages reflect the number of seedlings that had developed cotyledons on day 6 after sowing, normalized to the total number of seeds sown. Bars are means  $\pm$  SE of at least three plates containing 50 seeds each. Asterisks indicate significant differences ( $P < 0.05$ ) to the wild type. A photo of the seedlings is shown in Supplemental Figure 4 online.



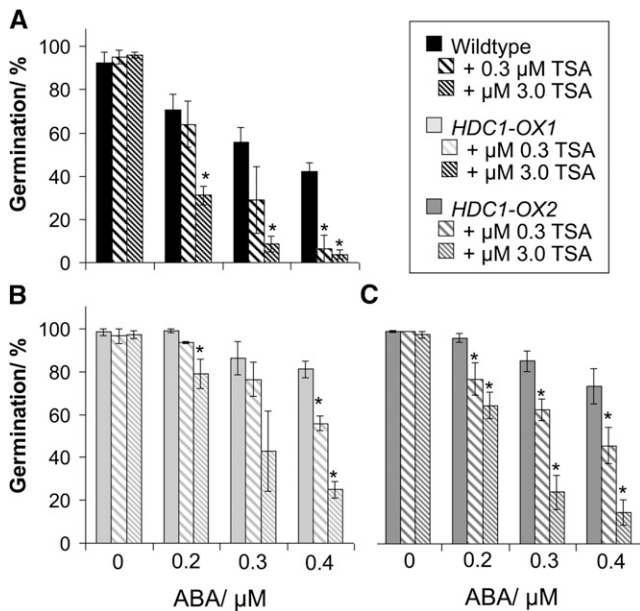


**Figure 6.** Histone Deacetylation Is Required for ABA Hyposensitivity.

Germination rates of *Arabidopsis* wild-type (**B**) and *HDC1*-overexpressing plants (**B**) and (**C**) on agar containing increasing concentrations of ABA with or without 0.3 or 3 μM histone deacetylation inhibitor TSA. Other details as in Figure 5.

this process, we subjected germinating seeds to the HDAC inhibitor trichostatin A (TSA). Unlike higher TSA concentrations tested before (Tanaka et al., 2008), the low micromolar concentrations of TSA applied in our experiments had no effect on seed germination in the absence of ABA (Figure 6). Nevertheless, TSA increased the ABA sensitivity of wild-type plants in a dose-dependent manner, with 0.3 μM producing a significant effect at 0.2 μM ABA and 3 μM TSA producing a significant effect at 0.4 μM ABA. Furthermore, addition of TSA increased ABA sensitivity of the *HDC1*-overexpressing lines. Thus, ABA sensitivity of germinating seeds and desensitization of seedlings toward ABA by *HDC1* overexpression depend on the catalytic activity of HDACs.

### *HDC1* Does Not Affect Vegetative Development but Is Required for Flowering

Several developmental phenotypes have been reported for HDAC mutants. For example, *hda6 hda19* double mutants display embryonic structures on mature leaves and do not repress embryonic-specific transcription factors, such as *LEAFY* *COTYLEDON1* (*LEC1*), *FUSCA3* (*FUS3*), and *ABA INSENSITIVE3* (*ABI3*) after germination (Tanaka et al., 2008). By contrast, leaves of *hdc1-1* plants were normal, and *LEC1* and *FUS3* were effectively repressed already 2 d after germination (DAG; see Supplemental Figure 4B online). *ABI3* transcript was still present at 2 DAG, with *hdc1-1* plants expressing higher levels and *HDC1-OX* plants expressing lower levels than wild-type plants, but was reduced to very low levels in all lines by 6 DAG. We conclude that in control

conditions, *HDC1* is not required for successful progression of seedlings into the vegetative growth phase.

During vegetative growth, leaf development was normal in *hdc1-1* and *HDC1-OX* plants. New leaves appeared at a similar rate in all lines (Figure 7A). When grown in long-day conditions, wild-type and *HDC1-OX* plants started to bolt within 4 weeks, whereas *hdc1-1* plants continued to produce rosette leaves and flowered ~2 weeks later (Figure 7B) at considerably higher rosette leaf number (Figure 7C). The flowering phenotype was reflected in a high transcript level of the flowering inhibitor *FLC* in *hdc1-1* knockout plants on day 28 compared with low levels in the wild-type and *HDC1-OX* plants (Figure 7D). It can be concluded that *HDC1* does not affect vegetative development but is required for the transition to the reproductive stage.

### *HDC1* Promotes Plant Growth

Despite normal vegetative development, *HDC1* mutant lines showed a clear growth phenotype (Figure 8). Differences in root length and leaf size started to appear within 2 weeks after germination (see Supplemental Figure 6 online) and led to significant differences of shoot and root weights in older plants, particularly when the vegetative growth phase was extended by applying short-day conditions (Figure 8). With a similar number of leaves,

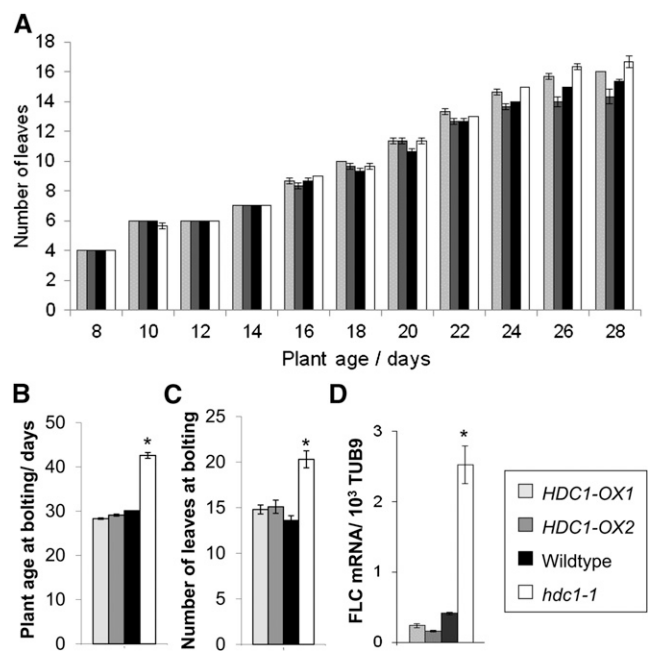


**Figure 7.** Knockout of *HDC1* Delays Flowering without Altering the Plastochron.

(A) Plastochron of wild-type (black), *hdc1-1* knockout (white), and *HDC1-OX* plants (gray) growing on soil in long-day conditions. Bars are means of three plants  $\pm$  SE. (B) Plant age at bolting. Bars are means  $\pm$  SE of 10 to 15 plants. (C) Number of leaves at bolting. Bars are means  $\pm$  SE of 10 to 15 plants. (D) *FLC* transcript levels on day 28. Bars are means  $\pm$  SE of three plants. Asterisks indicate differences to the wild type at  $P < 0.05$ .

4-week-old *HDC1-OX* plants had produced 20% more and *hdc1-1* plants had produced 10% less fresh weight than wild-type plants, and the differences increased to 50% (more or less weight) after 5 weeks (Figure 8A). All lines had a similar relative water content of  $92\% \pm 1\%$ ; hence, differences in fresh weight were primarily caused by differences in dry matter. Both *HDC1*-overexpressing lines showed enhanced growth, with *OX2* (*Ubi10*) being consistently slightly bigger than *OX1* (35S) plants. A positive correlation between *HDC1* expression level and growth was further confirmed in *hdc1-1:HDC1* complementation lines. Plant sizes and weights reflected the *HDC1* protein levels in the lines (Figure 8B).

*Arabidopsis* HDAC mutants have not been shown to have obvious growth phenotypes. We therefore reassessed growth of *hda6* knockdown (*axe1-5*) plants in our growth conditions. Indeed, *axe1-5* plants produced less fresh and dry weight than the corresponding wild-type plants (Col-0 DR5) despite slightly higher leaf number (see Supplemental Figure 7 online). By contrast, *HDA6*-overexpressing plants had similar weights as wild-type plants (see Supplemental Figure 5C online) and therefore did not phenocopy *HDC1*-overexpressing lines.

### HDC1 Alters Transcript Levels and Acetylation Status of Salt Stress-Regulated Genes

To examine a function of *HDC1* in transcriptional regulation, we treated 4-week-old hydroponically grown wild-type and mutant plants with 150 mM NaCl for 24 h and determined transcript levels of several known salt stress-responsive genes, including ABA biosynthesis genes ABA DEFICIENT1 (*ABA1*) and ABA DEFICIENT3 (*ABA3*), transcription factors RESISTANT TO DESSICATION29A/B (*RD29A/B*), dehydrin RESPONSIVE TO ABA18, and ABI FIVE BINDING PROTEIN3 (*AFP3*) (Yamaguchi-Shinozaki and Shinozaki, 2006). We found that after the salt treatment, transcript levels showed a consistent profile across the lines with higher levels in *hdc1-1* and/or lower levels in *HDC1-OX* plants than in wild-type plants (Figure 9). In control conditions, transcript levels of the genes were similarly low in all lines apart from *ABA1* transcript, which was increased in *hdc1-1*. Analysis of shoot ABA levels confirmed that ABA biosynthesis was efficiently induced by salt in all lines, but attained levels were slightly higher/lower in *hdc1-1/OX* lines (see Supplemental Figure 8 online). ABA receptor *PYR1-LIKE4* (*PYL4*; Lackman et al., 2011) and drought-repressed protein protease-like DROUGHT-REPPRESSED4 (*DR4*)

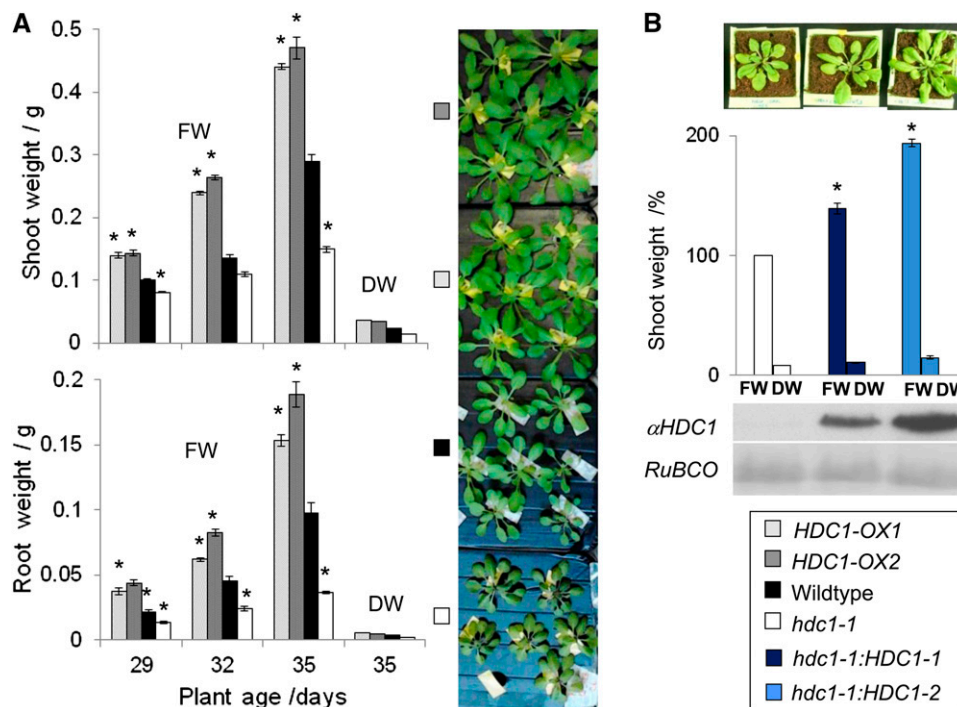


**Figure 8.** *HDC1* Promotes Vegetative Plant Growth.

**(A)** Shoot and root fresh weight (FW) of wild-type (black), *hdc1-1* knockout (white), and *HDC1 OX* plants (gray). Plants were grown hydroponically in short-day conditions. Bars show mean fresh weight of six plants  $\pm$  SE. Asterisks indicate difference to the wild type at  $P < 0.05$ . For determination of dry weights (DW), tissues of the six plants harvested on day 35 were pooled and dried. The combined weight was divided by the plant number. Appearance of the plants on day 35 is shown in the photo on the right.

**(B)** Shoot weights of *hdc1-1* knockout plants and of two independent complementation lines (genomic *HDC1* in *hdc1-1* background). Bars are means of five plants  $\pm$  SE, each compared with the *hdc1-1* plant grown in the same tray. The photo shows typical plant appearance (day 24, long-day conditions). Protein gel blot of leaf protein extract with *HDC1*-antibody ( $\alpha$ *HDC1*) reflects the amount of *HDC1* protein in the plants. Ponceau-stained ribulose-1, 5-bis-phosphate carboxylase/oxygenase (*RuBCO*) provides a loading control.

[See online article for color version of this figure.]

are examples of genes that are downregulated by osmotic stress (Kilian et al., 2007). We found that both genes were efficiently repressed by salt stress in all lines, but in control conditions, *hdc1-1* and *HDC-OX* plants produced higher and lower transcript levels than the wild type, respectively.

To assess whether and which of the observed transcriptional changes were a consequence of altered histone acetylation status, we performed anti-H3K9K14ac chromatin immunoprecipitation (ChIP)-quantitative PCR (qPCR) on regions encompassing the start codons of the above genes. For *ABA1*, *RD29B*, *PYL4*, and *DR4*, we recovered less ChIP-DNA from *HDC1-OX* plants and more from ChIP-DNA *hdc1-1* plants than from wild-type plants (Figure 10). By contrast, no change was found for *ABA3* (see Supplemental Figure 9 online), suggesting that the transcriptional changes in this gene are the result of positive feedback regulation through ABA (Barrero et al., 2006). The acetylation status of other genes remains to be tested. The results obtained here identify *ABA1*, *RD29B*, *PYL4*, and *DR4* as potentially direct targets of *HDC1*-facilitated histone deacetylation, and they provide a mechanistic explanation for the altered transcriptional responses of these genes in the mutants.

### The Growth-Enhancing Effect of *HDC1* Overexpression Is Maintained under Moderate Drought and Salt Stress

The combination of enhanced growth with lower expression of stress-inducible genes in *HDC1-OX* lines raised our curiosity

about the net outcome of these potentially counterproductive features on plant performance under water or salt stress. We therefore subjected *HDC1* mutant lines and wild-type plants to a controlled water-limiting regime in short-day conditions that started on day 14 and imposed a continuous relative soil water content of ~50% of the control condition for the remainder of the experiment (Figure 11A). Differences in growth between the lines were apparent in larger (*HDC1-OX*) and smaller (*hdc1-1*) rosette diameters of younger plants, recorded on days 14 and 28. In older plants, rosette diameters differed less due to maximal extension of the outer leaves, but significant differences of total shoot fresh and dry weights were found when the plants were harvested on day 40 (before flowering). In well-watered conditions, shoot fresh weights were ~20% higher in *HDC1-OX* plants and ~40% lower in *hdc1-1* plants than in wild-type plants. Limited water supply slowed the growth of all lines (by ~30% on day 28 and ~80% on day 40; see insets with absolute wild-type data in Figure 11A), yet *HDC1-OX* plants still produced significantly higher (~20%) biomass than wild-type plants, and *hdc1-1* knockout plants were still significantly smaller than wild-type plants (although the difference in fresh weight had narrowed to ~10%; Figure 11A).

In a second experiment, hydroponically grown plants were subjected for 6 d to salt stress (Figure 11B). Addition of 80 mM NaCl is a physiologically relevant sublethal salt stress dose for moderately salt-tolerant plants such as *Arabidopsis* (Wang et al., 2006) and did not cause severe chlorosis or desiccation over the course of this experiment (see photos in Figure 11B). However, the treatment reduced shoot water content (from 92% ± 1% to

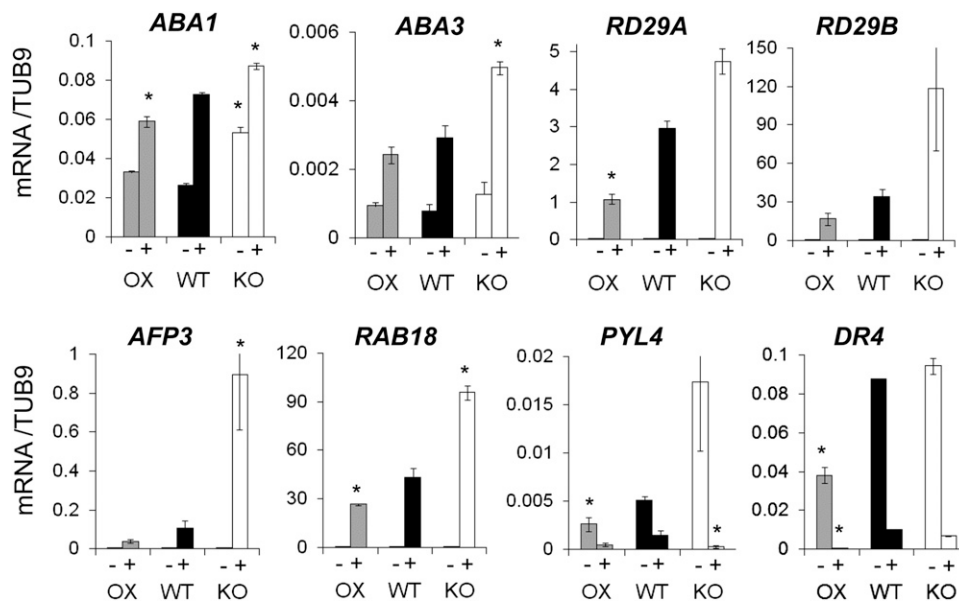


**Figure 9.** *HDC1* Knockout/Overexpression Deregulates Salt-Responsive Genes.

Transcript levels of salt-responsive genes in the wild type (WT; black), *hdc1-1* knockout (KO; white), and *HDC1* overexpressing line (OX; gray). Plants were grown for 4 weeks in short-day conditions and subjected (+) or not (–) to 150 mM NaCl for 24 h in hydroponics. mRNA was pooled from three independently treated plant batches of five plants each. Each replicate treatment resulted in a significant increase of ABA (see Supplemental Figure 8 online). Transcript levels were normalized to those of *tubulin 9* (*TUB9*). Bars are means of four technical qPCR replicates ± SE. Asterisks indicate significant differences to the wild type ( $P < 0.05$ ). *RAB18*, RESPONSIVE TO ABA18.



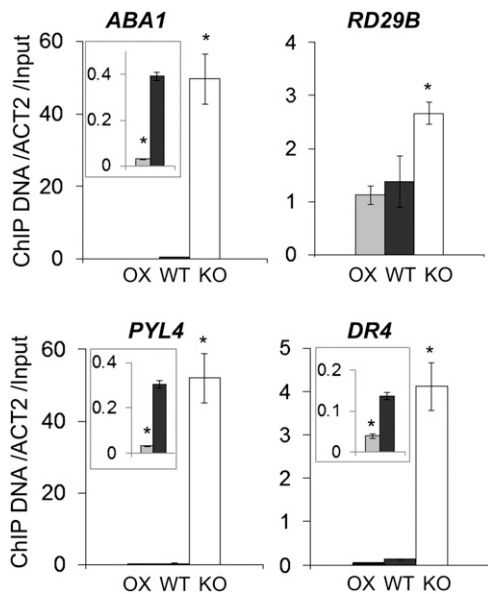


**Figure 10.** HDC1 Determines H3K9/K14 Acetylation Status of ABA1, DR4, PYL4, and RD29B.

Relative amounts of DNA associated with acetylated H3K9/K14 for ABA1, DR4, PYL4, and RD29B as determined by ChIP-qPCR in wild-type (WT; black), *hdc1-1* knockout (KO; white), and *HDC1*-overexpressing (OX; gray) plants. Leaf tissue was pooled from 4-week-old plants grown in three independent batches 12 plants each. Chromatin extracted and immunoprecipitated with anti-H3K9K14Ac. qPCR-amplified ChIP-DNA was normalized to *ACT2* and to input DNA (chromatin before immunoprecipitation). Bars are means of four technical qPCR replicates  $\pm$  SE. Asterisks indicate significant differences to the wild type ( $P < 0.05$ ).

86%  $\pm$  1% after 6 d) and slowed growth in all lines (compared with data for control plants in Figure 8). Importantly, salt-stressed *HDC1*-OX continued to produce significantly more root and shoot biomass than the wild type and *hdc1-1* plants remained smaller. Thus, under moderate salt stress, the growth advantage of *HDC1* overexpression is maintained despite lower responsiveness of salt-inducible genes.

## DISCUSSION

### Plant *HDC1*-Type Proteins Have Extended from Smaller *Rxt3* Proteins in Fungi and Algae

Here, we presented the functional characterization of a plant gene with an important role in fundamental life processes, including germination, vegetative growth, and flowering. The identification of *HDC1* was based on its partial homology with the yeast gene *Rxt3*. Present in fungi, protozoa, and plants, but not in animals and humans, *Rxt3*/*HDC1* homologs are potentially interesting targets for drug and crop development, but their role in non-plant species has remained obscure. In yeast, *Rxt3* coelutes with other proteins of the large Rpd3 histone deacetylation complex, but the protein is neither required for deacetylation of known Rpd3 targets nor for

in vitro reassembly of a minimal functional Rpd3 complex (Carrozza et al., 2005a; Chen et al., 2012). The protein sequence of *Rxt3* does not contain any regions with known function in enzymatic activity or histone/DNA binding properties. Nevertheless, the *Rxt3* part and its core signature are well conserved in the plant proteins (Figure 1B). Clearly, a detailed structure-function analysis of this class of proteins is long overdue. The ABA-hypersensitive germination of *Arabidopsis hdc1-1* mutants provides a quick functional assay for such studies.

*HDC1*-like proteins in land plants are considerably larger than the ancestral *Rxt3* proteins (Figure 1B), suggesting additional functions or regulatory sites. Publicly available microarray data indicates that *HDC1* transcript is unchanged across a large number of environmental conditions, including salt, drought, and pathogen infection (eFP browser in The Arabidopsis Information Resource; Winter et al., 2007). Whether the *HDC1* protein is subject to posttranslational regulation and under which conditions should now be explored. The fact that sequence extension from *Rxt3* to *HDC1* occurred between algae and land plants is interesting as it coincides with the need of plants to adapt to water stress on land and with the promotion of ABA from growth regulator to plant hormone (Takezawa et al., 2011). It is tempting to speculate that the development of *HDC1* as an ABA-stat made an important contribution to this evolutionary progress.

### *HDC1* Is a Titratable Component of Histone Deacetylation Complexes

*hdc1-1* knockout phenocopied knockout/knockdown of HDACs HDA6 or HDA19 with respect to ABA-sensitive germination and flowering (Figures 5 and 7). The fact that *hdc1* knockout inhibited both of these HDAC-mediated processes (Song et al., 2005; Yu et al., 2011) although they involve different repressors (ETHYLENE RESPONSE FACTOR7 and FLOWERING LOCUS D, respectively) and different transcriptional targets (ABA-inducible genes and FLC, respectively) positions *HDC1* action upstream of the respective signaling pathways. A third phenotype consisting in reduced vegetative growth was also found to be shared between *hdc1-1* and *hda6* (*axe1-5*) mutants (Figure 8; see Supplemental Figure 7 online), thus adding further evidence for a closely related function. However, *hdc1* knockout did not reproduce aberrant developmental phenotypes observed in *hda6 hda19* double mutants (Tian and Chen, 2001; Tanaka et al., 2008) suggesting that basal activity of at least one of the two HDACs is maintained in the absence of *HDC1*.

We further showed that *HDC1* physically interacts with HDA6 and HDA19 and is required for deacetylation of Lys 9 and 14 in histone 3 (H3K9K14) (Figures 3, 4, and 10). Based on its general occurrence as a single-copy gene and its ubiquitous expression within the plant, *HDC1* is likely to function as a universal scaffolding protein that enhances the apparent HDAC activity by stabilizing the interaction of the enzymes with the substrate or with other regulatory proteins (Figure 12). In yeast and animals, interaction of HDACs with downstream repressors is achieved through corepressor proteins, such as SIN3, and in Arabidopsis,

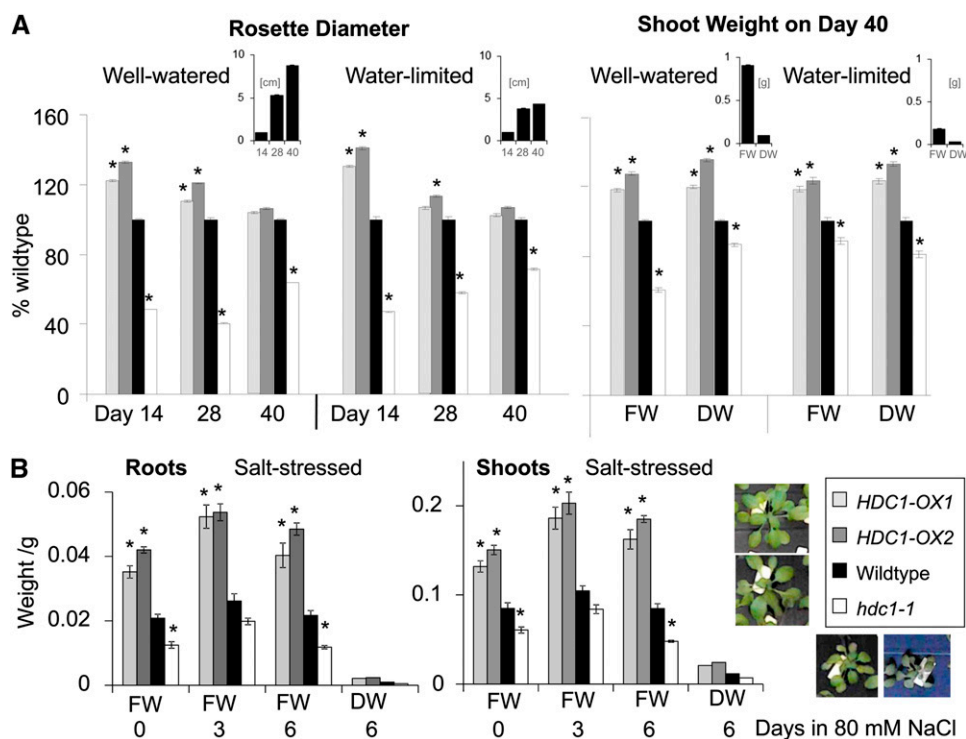


**Figure 11.** HDC1 Increases Plant Growth in Well-Watered and in Water-Limited Conditions.

**(A)** Rosette diameter and shoot weights (fresh weight [FW]; dry weight [DW]) of wild-type (black), *hdc1-1* knockout (white), and *HDC1 OX* plants (gray). Plants were grown on soil in short-day conditions. The water-limited regime consisted of reducing water supply from day 14 to achieve a continuous relative soil water content of ~50% of the control condition until the end of the experiment at day 40. Bars are means  $\pm$  SE of at least 24 plants. Asterisks indicate differences to the wild type at  $P < 0.05$ . Insets show absolute values for the wild type in each condition.

**(B)** Root and shoot weights of hydroponically grown plants growing in nutrient solution with 80 mM NaCl. Plant age at the beginning of the experiment was 29 d (short-day conditions). The first time point is 6 h after salt application. Control plants grown in parallel without salt are shown in Figure 8. Bars are mean fresh weights  $\pm$  SE of six plants per line. Asterisks indicate differences to the wild type at  $P < 0.05$ . For determination of dry weight, the tissues of six plants were pooled. Photos show plants of each line after 6 d in 80 mM NaCl.

[See online article for color version of this figure.]

one of six SIN3-like proteins in *Arabidopsis* has been shown to interact with both HDA19 and ERF7 (Song et al., 2005). Our quantitative BiFC assay showed SIN3 does not directly interact with HDC1, suggesting that HDC1 operates in histone binding rather than DNA binding. In yeast, Rxt3 and the histone binding protein Pho23 form a submodule that is linked to the core complex via another functionally uncharacterized protein, Rxt2 (Carrozza et al., 2005b). Both Pho23 and Rxt2, as well as other putative members of the complex, have multiple homologs in *Arabidopsis*. A systematic dissection of HDAC multiprotein complexes in plants is now needed to explore how HDC1 affects their composition and stability in vivo.

Overexpression of *HDC1* produced significant phenotypes both at the physiological level (Figures 5 and 8) and at the molecular level (Figures 9 and 10), which were opposite to those of *hdc1-1* mutants and hence directly linked to HDC1. To date, no phenotypes have been reported for overexpression of *HDA6*, and our own analysis of *35S:HDA6* lines did not reveal any phenotypic differences to the wild type (see Supplemental Figure 5 online).

Overexpression of an *HDA19* homolog in rice, on the other hand, increased growth but also produced a range of developmental abnormalities that did not occur in *HDC1*-overexpressing plants. Thus, indirect manipulation of HDAC activity via titration of *HDC1* expression levels provides a means to effectively regulate plant growth and stress sensitivity without developmental side effects (see also below).

From a mechanistic point of view, opposite effects of knockout and overexpression of *HDC1* indicate that the amount of *HDC1* protein is a limiting factor in the histone deacetylation machinery that determines the rate and sensitivity of downstream processes (Figure 12). Viability and normal development of *hdc1* mutants also suggests that the role of *HDC1* is in fine-tuning rather than essential maintenance.

#### HDC1 Titrates Transcript Levels of Stress-Responsive Genes

In accordance with a repressive function of histone deacetylation, we found that transcript levels of several known

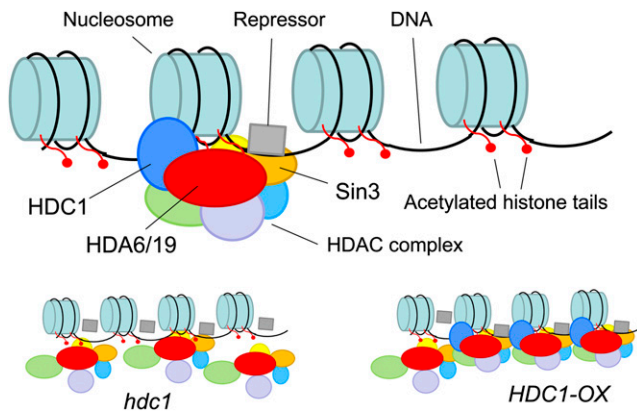


**Figure 12.** Working Model for HDC1 Function.

Based on protein interaction studies and physiological phenotypes, it is proposed that HDC1 is a critical component of multiprotein complexes that mediate histone deacetylation. HDC1 enhances the repressive effect of histone deacetylation on transcription, probably by stabilizing the complex and/or its association with the chromatin. Knockout of HDC1 destabilizes the complex and therefore phenocopies knockout/knockdown of interacting HDACs. The fact that overexpression of HDC1 is also phenotypically effective suggests that other essential components of the complex are present in abundance and that their action can be further enhanced by increasing the amount of HDC1. Note that a spatial enhancement of active complexes is shown here for simplicity, but the effect of HDC1 overexpression is likely to be kinetic through an increase in the frequency/duration of chromatin binding at a given site.

[See online article for color version of this figure.]

stress-responsive genes were increased in *hdc1-1* knockout plants and/or decreased in *HDC1-OX* plants. Determination of H3K9K14 acetylation levels identified at least four of these genes as direct targets of HDC1-facilitated deacetylation. HDC1 knockout/overexpression affected both stress-inducible genes, such as *Rd29B* and *ABA1*, and stress-repressed genes, such as *DR4* and *PYL4*. Neither of the genes featured in a previously published list of genes that are deregulated in *axe1-5* mutants (To et al., 2011). However, this list was limited to genes with more than threefold changes in control conditions. The transcriptional changes caused by HDC1 knockout/overexpression were relatively small despite very large changes in histone acetylation levels in some of the genes (Figure 10), indicating that additional levels of regulation limit the effects of histone deacetylation on transcript levels. This could also explain the low number of deregulated genes identified in *axe1-5* mutants. Based on our data, we propose a model in which HDC1-facilitated histone deacetylation increases the amount of stimulus (e.g., ABA) and activator (e.g., transcription factor) required for derepression of a gene upon stress, thereby reducing its stress sensitivity (see Supplemental Figure 10A online). Absence of HDC1 lowers the amount of stimulus required for derepression but is not sufficient to activate transcription when stimulus and activator are absent (i.e., in control conditions). In the case of a stress-repressed gene, HDC1 decreases the efficiency of a given amount of constitutive activator, thereby

reducing transcript levels (see Supplemental Figure 10B online). Whether or not this has an effect on downregulation upon stress will then depend on whether the stress-induced repressor acts upstream or downstream of the constitutive activator. This working model needs now to be confirmed and refined through genome-wide analysis of transcript and histone acetylation profiles of HDC1 mutants in a range of environmental conditions.

### HDC1 Still Promotes Growth under Moderate Drought and Salt Stress

The finding that HDC1 genetically couples decreased stress sensitivity with enhanced growth gave us the opportunity to contribute experimental evidence to the ongoing discussion of what constitutes drought tolerance. A recent correspondence to *Nature Biotechnology* (Skirycz et al., 2011) ascribed the relatively low success rate of translating fundamental *Arabidopsis* research into crop improvement to the fact that the former had focused on improving plant survival under desiccation (e.g., by overexpressing ABA targets), while the latter required better growth under mild drought conditions. The authors supported their claim by showing that in a preselected *Arabidopsis* mutant population plant growth under mild drought stress was positively correlated with plant growth in well-watered conditions, independently of drought survival phenotypes (Skirycz et al., 2011). Our results with *HDC1* mutants (Figure 11) support the importance of growth under reduced irrigation and moderate salinity and go a step further by showing that a growth advantage occurring in well-watered conditions can be maintained in moderate stress conditions even if directly coupled with attenuated induction of dehydration-inducible genes. At this moderate stress, the lines showed no or little difference in stress sensitivity (see Supplemental Figure 11 online). Based on the well-known role of ABA for plant survival under desiccation, it can be expected that *hdc1* mutants gain an advantage under more severe stress. How exactly biomass production (higher in *HDC1-OX*) and ABA-triggered survival strategies (more pronounced in *hdc1*) contribute to net yield in different stress situations should be addressed in the future by monitoring biomass, relative water content, and poststress recovery in *hdc1* and *HDC1-OX* plants over a wide range of increasing stress severity.

In conclusion, the discovery of HDC1 adds a quantitative element to the histone deacetylation machinery in plants. Several physiological outputs of histone deacetylation that are highly relevant for plant biotechnology can be titrated through HDC1 expression, without producing any of the morphological abnormalities observed for manipulation of HDACs in *Arabidopsis*, rice, and maize (Tian and Chen, 2001; Jang et al., 2003; Zhou et al., 2005; Rossi et al., 2007; Tanaka et al., 2008). Thus, HDC1 opens avenues to exploit epigenetic regulation for crop improvement without risking unwanted side effects caused by interference with fundamental roles of chromatin modifications in tissue differentiation. The growth-enhancing effect of HDC1 overexpression in both well-watered and water-limited conditions is particularly promising in the context of sustainable, water-efficient agriculture.

## METHODS

### Plant Materials

All transgenic lines for HDC1 were generated in our laboratory in *Arabidopsis thaliana* Col-0 background. The stable homozygous knockout line *hdc1-1* was obtained from progeny of GABI-Kat 054G03. Stable, homozygous complementation lines were identified from the progeny of *hdc1-1* plants transformed with genomic *HDC1*, including the native promoter (see cloning procedures). Stable, homozygous *HDC1*-overexpressing lines were generated from the progeny of wild-type Col-0 plants transformed with *HDC1* under the control of 35S or Ubiquitin-10 promoters (see cloning procedures). Seeds for 35S:*HDA6* (Gu et al., 2011) and *axe1-5* (Probst et al., 2004) were kindly provided by Yuehui He and Ortrun Mittelsten Scheid, respectively.

### Growth Conditions and Treatments

All experiments were performed in controlled growth rooms at a temperature of 20 to 22°C and a light intensity of 120 to 150 μmol PAR. Plants were grown either in long days (16-h light) or in short days (10-h light) as indicated in text and figure legends. Seeds of *Arabidopsis* wild-type and transgenic lines were sterilized, stratified, and germinated on soil or on agar plates. Agar plates contained half-strength Murashige and Skoog media with 1% Suc and 0.8% agar at pH 5.7. For germination assays, media were supplemented with NaCl, ABA (Sigma-Aldrich), PAC (Fluka), or TSA (Sigma-Aldrich) at the concentrations given in the figures. Germination rate was scored on day 6 after sowing by counting seedlings that had developed green cotyledons. Experiments with adult plants were performed on soil or in hydroponic culture. For the latter, seeds were germinated on agar plates and 2- to 3-week-old seedlings were placed in perforated lids of black 0.7-liter plastic containers. The growth medium consisted of a minimal sufficient nutrient medium (Kellermeier et al., 2013). For salt treatment, NaCl powder was stirred directly into the growth container to obtain the desired concentration (as stated in the figures). Control media were stirred without adding NaCl. For controlled drought experiments, plants were grown on soil in pots according to a randomized design. Using previously reported methodology (Granier et al., 2006; Skiryicz et al., 2011), controlled watering was used to impose moderate water stress. After 14 d of plant growth in well-watered soil, watering was reduced so that the relative soil water content of the stressed plants was maintained at 50% of the normal watering regime. Control plants were watered normally.

### Sequence Alignment

BLASTp searches were performed with the predicted amino acid sequence of HDC1 against the database of nonredundant protein sequences at the National Center for Biotechnology Information using default parameters (matrix BLOSUM62, existence 11, and extension 1). Representative sequences from different kingdoms (listed in Supplemental Data Set 1 online) were subsequently aligned using the COBALT tool (Papadopoulos and Agarwala, 2007) with default parameters (gap penalties  $-11/-1$  and end-gap penalties  $-5/-1$  for opening/extension). The extracted cluster dendrogram (COBALT tree) reflects the overall similarity between the aligned sequences (note that this is not a phylogenetic tree). An additional sequence alignment was performed with the full-length sequence of the yeast Rxt3 protein and the corresponding parts in the *Arabidopsis* and *Brachypodium distachyon* HDC1 proteins.

### Cloning Procedures

Entry clones with full-length *HDC1*, *HDA6*, *HDA19*, and *SIN3* with or without stop codon were generated by PCR amplification using primers that contained attB1 and attB2 sites or attB3 and attB4 as 5' modifications. Gel-purified PCR products were introduced into pDONR207/

221 (Life Technologies) using BP-clonase II according to the manufacturer's instructions and transferred to destination vectors by recombination using LR-clonase II (Life Technologies). The reaction product was used to transform Top10 bacterial cells. Antibiotic marker-resistant colonies were isolated and verified by restriction digest analysis and sequencing. The following plasmids were generated and used in this study: 35S:*HDA6/HDA19*-RFP in pB7RWG2, *HDC1* (646 bp upstream) promoter in pMDC163, *HDC1* genomic DNA (including 646-bp upstream sequence) in pMDC123, 2X35S:*HDC1* in pMDC032 (Curtis and Grossniklaus, 2003), Ubi10:*HDC1* in pUB-Dest, 35S:GFP-*HDC1* in pH7WGF2 (Karimi et al., 2002), Ubi10:GFP-*HDC1* pUBN-GFPDest (Grefen et al., 2010), 35S:nYFP-*HDC1*/cYFP-*HDA6/HDA19/SIN3* in pBiFCt-2in1-NN, and 35S:nYFP-*SIN3*/cYFP-*HDA19* in pBiFCt-2in1-NN (Grefen and Blatt, 2012).

### Antibodies

*HDC1* antibody was raised in rabbit (Agriser), using a synthetic peptide matching amino acids 341 to 356 in the *HDC1* sequence, and affinity purified. An extra Cys was added to the N terminus to improve binding capacity. H3K9/K14Ac and H3 antibodies were purchased from Diagenode (pAb-005-044) and Abcam (ab1791). His-tag antibody was obtained from New England Biolabs (No. 2366).

### Plant Transformation

Plasmids were inserted by heat shock into *Agrobacterium tumefaciens* strain GV3101 pMP90 (Koncz and Schell, 1986). *Agrobacterium*-mediated transformation of *Arabidopsis* was performed by the floral dip method (Clough and Bent, 1998). Homozygous T2 progenies were used for germination tests. *Agrobacterium*-mediated transient transformation of *Nicotiana tabacum* and *Nicotiana benthamiana* was achieved by leaf infiltration (Geelen et al., 2002). For ratiometric BiFC assays and colocalization studies, each construct was coexpressed with p19 protein of tomato bushy stunt virus, encoding for a suppressor of gene silencing (Voinnet et al., 2003).

### PCR

Total genomic DNA was extracted according to Edwards et al. (1991). All PCR reactions were performed with 0.4 units of Taq polymerase (Promega). Total RNA was extracted using hot phenol. cDNA was obtained with the Quantitect reverse transcription kit (Qiagen) following the manufacturer's procedure. Quantitative RT-PCR was performed on an MX3000 sequence detection system (Agilent) with Brilliant III UltraFast SYBR QPCR Master Mix (Agilent). Primer sequences are provided in Supplemental Table 1 online. Reactions were performed in four technical replicates on three biological replicates.

### ChIP

Chromatin extraction and ChIP were performed using published protocols (Gendrel et al., 2002; Saleh et al., 2008; Sani et al., 2013). Tissue samples were incubated in 1% (w/v) formaldehyde for 15 min under vacuum. To stop cross-linking, 125 mM Gly was added, and tissues were rinsed, blotted dry, and frozen. Chromatin extracts were incubated with antibody against H3K9/K14Ac (Diagenode pAb-005-044) following the manufacturer's instructions. Immunoprecipitated chromatin-DNA (IP-DNA) and input chromatin-DNA were reverse cross-linked, and residual protein was removed by proteinase K treatment. DNA was extracted with phenol and chloroform and ethanol precipitated. DNA was resuspended and purified by MinElute Reaction Cleanup kit (Qiagen). Before proceeding to ChIP-qPCR, DNA samples were amplified using GenomePlex Complete Whole

Genome Amplification (WGA2; Sigma-Aldrich) following the manufacturer's protocol. As a quality control for successful ChIP, existence or absence of sequences previously found to be associated (positive control) or not (negative control) with H3K9K14Ac (Zhou et al., 2010; To et al., 2011) in the ChIP samples was confirmed by PCR. Supplemental Table 1 online lists primer pairs and positions of the amplified regions for Actin2 (positive control), AT1G37110 (negative control), and the tested genes.

### Protein Extraction and Protein Gel Blotting

Nuclei-enriched protein extracts were prepared according to a published protocol (Gendrel et al., 2002). The chromatin was extracted twice with 0.4 M H<sub>2</sub>SO<sub>4</sub> and proteins precipitated with 20% trichloroacetic acid. All buffers were supplemented with 100 mM PMSF and proteinase inhibitors (Complete Mini; Roche). Samples were boiled and loaded onto SDS-PAGE gels. After transfer to polyvinylidene difluoride membrane (IPVH00010; Millipore), Ponceau S staining (P3504; Sigma-Aldrich) was performed. *HDC1* antibody was incubated overnight in a dilution of 1:4000. Secondary rabbit antibody conjugated with horseradish peroxidase (Roche) was incubated with the membrane for at least 1 h. Proteins were detected using the ECL+ system (RPN2132; Amersham).

### Production of Recombinant Tagged Protein and GST Pull-Down Assays

GST- or His-tagged proteins were expressed in *Escherichia coli* BL21 cells. Following induction with 1 mM isopropyl β-D-1-thiogalactopyranoside, cells were harvested and sonicated in lysis buffer. The soluble *HDC1*-His, GST-HDA6, and GST-HDA19 proteins were affinity-purified using the nickel-nitrilotriacetic acid (Sigma-Aldrich) and Glutathione-Sepharose resin (GE Healthcare) according to the manufacturer's instructions. For pull-down assays, GST-tagged proteins were bound to Glutathione-Sepharose resin and applied to a microcolumn. Recombinant *HDC1*-His or nuclei-enriched plant lysates (Gendrel et al., 2002) were combined with 1 × protein inhibitor (Complete Mini, 11836153001; Roche) in Tris(hydroxymethyl)aminomethane-NaCl buffer. Samples were incubated overnight on ice. After several washes, pulled-down protein was eluted in 1 × Laemmli buffer.

### GUS Assay

Plant tissues from independent primary transformants expressing GUS under control of the *HDC1* promoter were infiltrated in a solution containing 2 mM 5-Bromo-4-chloro-1H-indol-3-yl β-D-glucopyranosiduronic acid. The samples were incubated overnight at 37°C, followed by ethanol washes to remove excess dye. Photos were taken on a stereomicroscope (MSA 166305; Wild Heerbrugg).

### Confocal Microscopy

Fluorescence in tobacco epidermal cells was assessed 2 d after infiltration using a CLSM-510-META-UV confocal microscope (Zeiss). For single protein localization, GFP fluorescence was excited at 488 nm with light from an argon laser and collected after passage through an NFT545 dichroic mirror with a 505-nm long-pass filter. For colocalization experiments, GFP fluorescence was collected with a 505- to 530-nm band-pass filter. RFP fluorescence was excited at 543 nm with light from a helium neon laser and was collected after passage through an NFT545 dichroic mirror and a 560- to 615-nm band-pass filter. YFP fluorescence was excited at 514 nm with light from an argon laser and was collected using lambda mode between 520 and 550 nm. Colocalization plane and line scans were evaluated using Zeiss LSM 510 AIM software (v3.2).

### Determination of ABA Content

ABA in methanol extracts from dried leaf sample was quantified by liquid chromatography–mass spectrometry (Page et al., 2012) at the University

of Exeter Mass Spectrometry Facility (Exeter, UK) using 1200 series HPLC (Agilent Technologies; 3.5 μm, 2.1 × 150-mm Eclipse Plus C18 column) and a 6410B enhanced sensitivity triple quadrupole mass spectrometer (Agilent Technologies). [<sup>2</sup>H<sub>6</sub>] (+)-*cis,trans*-ABA (Chemlm) was included as a standard.

### Accession Numbers

Sequence data from this article can be found in the GenBank/EMBL libraries and in The Arabidopsis Information Resource under the following accession numbers: ABA1, AT5G67030; ABA3, AT1G16540; ABI3, AT3G24650; AFP3, AT3G29575; DR4, AT1G73330; FLC, AT5G10140; FUS3, AT3G26790; *HDC1*, AT5G08450; HDA6, AT5G63110; HDA19, AT4G38130; LEC1, AT1G21970; PYL4, AT2G38310; RESPONSIVE TO ABA18, AT5G66400; RESPONSIVE TO DESSICATION29, AAT1G16540; RD29B, AT5G52300; and SIN3 (also called SIN3-LIKE3), AT1G24190.

### Supplemental Data

The following materials are available in the online version of this article.

**Supplemental Figure 1.** Colocalization of *HDC1* with HDA6 and HDA19 within Nuclei of Transiently Expressing Tobacco Epidermis Cells.

**Supplemental Figure 2.** Confirmation of *hdc1-1* Knockout and *HDC1*-Overexpressing Lines.

**Supplemental Figure 3.** Salk150126 and Sail1263E05 Are Not *hdc1* Knockouts.

**Supplemental Figure 4.** Without ABA, *HDC1* Does Not Alter Germination or Progression of Seedlings to Vegetative Stage.

**Supplemental Figure 5.** *HDA6* Overexpression Does Not Affect Germination or Growth.

**Supplemental Figure 6.** Root and Leaf Growth Phenotypes in Young Plants.

**Supplemental Figure 7.** *HDA6* Knockdown Affects Plant Growth without Delaying Leaf Development.

**Supplemental Figure 8.** *HDC1* Has a Small Effect on ABA Content after Salt Treatment.

**Supplemental Figure 9.** *HDC1* Alters H3K9K14 Acetylation Levels in ABA1 but Not ABA3.

**Supplemental Figure 10.** Scenarios for the Effects of *HDC1* on ABA-Dependent Gene Expression.

**Supplemental Figure 11.** Effects of *HDC1* Expression on Stress Sensitivity during Vegetative Growth.

**Supplemental Table 1.** Primers for Genotyping gDNA.

**Supplemental Data Set 1.** Alignment of *HDC1* and Rxt3 Sequences from Different Organisms.

### ACKNOWLEDGMENTS

We thank Amparo Ruiz-Prado and Naomi Donald (University of Glasgow) for horticultural assistance. We thank Yuehui He (National University of Singapore), Ortrun Mittlesten Scheid (Gregor Mendel Institute Vienna), and Christopher Grefen (University of Glasgow) for supplying seeds and vectors. We thank Hannah Florance and Nick Smirnov from the Exeter Mass Spectrometry Facility for measuring ABA levels. We thank all members of the Glasgow laboratory for constructive comments on the article. The project was funded by the Leverhulme Trust and by Bayer CropScience.



## AUTHOR CONTRIBUTIONS

G.P., M.A.L.-V., M.A.H., and A.A. designed the research. G.P., M.A.L.-V., C.C., E.S., V.G., C.V., and F.K. performed the experiments and analyzed the data. A.A. wrote the article.

Received June 15, 2013; revised August 23, 2013; accepted August 28, 2013; published September 20, 2013.

## REFERENCES

- Barrero, J.M., Rodríguez, P.L., Quesada, V., Piqueras, P., Ponce, M.R., and Micol, J.L.** (2006). Both abscisic acid (ABA)-dependent and ABA-independent pathways govern the induction of NCED3, AAQ3 and ABA1 in response to salt stress. *Plant Cell Environ.* **29**: 2000–2008.
- Berger, S.L.** (2007). The complex language of chromatin regulation during transcription. *Nature* **447**: 407–412.
- Carrozza, M.J., Florens, L., Swanson, S.K., Shia, W.J., Anderson, S., Yates, J., Washburn, M.P., and Workman, J.L.** (2005a). Stable incorporation of sequence specific repressors Ash1 and Ume6 into the Rpd3L complex. *Biochim. Biophys. Acta* **1731**: 77–87, discussion 75–76.
- Carrozza, M.J., Li, B., Florens, L., Suganuma, T., Swanson, S.K., Lee, K.K., Shia, W.J., Anderson, S., Yates, J., Washburn, M.P., and Workman, J.L.** (2005b). Histone H3 methylation by Set2 directs deacetylation of coding regions by Rpd3S to suppress spurious intragenic transcription. *Cell* **123**: 581–592.
- Chen, L.T., Luo, M., Wang, Y.Y., and Wu, K.Q.** (2010). Involvement of *Arabidopsis* histone deacetylase HDA6 in ABA and salt stress response. *J. Exp. Bot.* **61**: 3345–3353.
- Chen, L.T., and Wu, K.Q.** (2010). Role of histone deacetylases HDA6 and HDA19 in ABA and abiotic stress response. *Plant Signal. Behav.* **5**: 1318–1320.
- Chen, X.F., Kuryan, B., Kitada, T., Tran, N., Li, J.Y., Kurdistani, S., Grunstein, M., Li, B., and Carey, M.** (2012). The Rpd3 core complex is a chromatin stabilization module. *Curr. Biol.* **22**: 56–63.
- Clough, S.J., and Bent, A.F.** (1998). Floral dip: A simplified method for *Agrobacterium*-mediated transformation of *Arabidopsis thaliana*. *Plant J.* **16**: 735–743.
- Curtis, M.D., and Grossniklaus, U.** (2003). A Gateway cloning vector set for high-throughput functional analysis of genes in planta. *Plant Physiol.* **133**: 462–469.
- Daszkowska-Golec, A.** (2011). *Arabidopsis* seed germination under abiotic stress as a concert of action of phytohormones. *OMICS* **15**: 763–774.
- Edwards, K., Johnstone, C., and Thompson, C.** (1991). A simple and rapid method for the preparation of plant genomic DNA for PCR analysis. *Nucleic Acids Res.* **19**: 1349.
- Finkelstein, R., Reeves, W., Ariizumi, T., and Steber, C.** (2008). Molecular aspects of seed dormancy. *Annu. Rev. Plant Biol.* **59**: 387–415.
- Geelen, D., Leyman, B., Batoko, H., Di Sansebastiano, G.P., Moore, I., and Blatt, M.R.** (2002). The abscisic acid-related SNARE homolog NtSyr1 contributes to secretion and growth: Evidence from competition with its cytosolic domain. *Plant Cell* **14**: 387–406. Erratum. *Plant Cell* **14**: 963.
- Gendrel, A.V., Lippman, Z., Yordan, C., Colot, V., and Martienssen, R.A.** (2002). Dependence of heterochromatic histone H3 methylation patterns on the *Arabidopsis* gene DDM1. *Science* **297**: 1871–1873.
- Granier, C., et al.** (2006). PHENOPSIS, an automated platform for reproducible phenotyping of plant responses to soil water deficit in *Arabidopsis thaliana* permitted the identification of an accession with low sensitivity to soil water deficit. *New Phytol.* **169**: 623–635.
- Grefen, C., and Blatt, M.R.** (2012). A 2in1 cloning system enables ratiometric bimolecular fluorescence complementation (rBIFC). *Biotechniques* **53**: 311–314.
- Grefen, C., Donald, N., Hashimoto, K., Kudla, J., Schumacher, K., and Blatt, M.R.** (2010). A ubiquitin-10 promoter-based vector set for fluorescent protein tagging facilitates temporal stability and native protein distribution in transient and stable expression studies. *Plant J.* **64**: 355–365.
- Gu, X.F., Jiang, D.H., Yang, W.N., Jacob, Y., Michaels, S.D., and He, Y.H.** (2011). *Arabidopsis* homologs of retinoblastoma-associated protein 46/48 associate with a histone deacetylase to act redundantly in chromatin silencing. *PLoS Genet.* **7**: e1002366.
- Hollender, C., and Liu, Z.C.** (2008). Histone deacetylase genes in *Arabidopsis* development. *J. Integr. Plant Biol.* **50**: 875–885.
- Jang, I.C., Pakh, Y.M., Song, S.I., Kwon, H.J., Nahm, B.H., and Kim, J.K.** (2003). Structure and expression of the rice class-I type histone deacetylase genes OsHDAC1-3: OsHDAC1 overexpression in transgenic plants leads to increased growth rate and altered architecture. *Plant J.* **33**: 531–541.
- Karimi, M., Inzé, D., and Depicker, A.** (2002). GATEWAY vectors for *Agrobacterium*-mediated plant transformation. *Trends Plant Sci.* **7**: 193–195.
- Kellermeier, F., Chardon, F., and Amtmann, A.** (2013). Natural variation of *Arabidopsis* root architecture reveals complementing adaptive strategies to potassium starvation. *Plant Physiol.* **161**: 1421–1432.
- Kilian, J., Whitehead, D., Horak, J., Wanke, D., Weinl, S., Batistic, O., D'Angelo, C., Bornberg-Bauer, E., Kudla, J., and Harter, K.** (2007). The AtGenExpress global stress expression data set: Protocols, evaluation and model data analysis of UV-B light, drought and cold stress responses. *Plant J.* **50**: 347–363.
- Kim, J.M., To, T.K., and Seki, M.** (2012). An epigenetic integrator: new insights into genome regulation, environmental stress responses and developmental controls by histone deacetylase 6. *Plant Cell Physiol.* **53**: 794–800.
- Koncz, C., and Schell, J.** (1986). The promoter of TL-DNA gene 5 controls the tissue-specific expression of chimeric genes carried by a novel type of *Agrobacterium* binary vector. *Mol. Gen. Genet.* **204**: 383–396.
- Kouzarides, T.** (2007). Chromatin modifications and their function. *Cell* **128**: 693–705.
- Kurdistani, S.K., and Grunstein, M.** (2003). Histone acetylation and deacetylation in yeast. *Nat. Rev. Mol. Cell Biol.* **4**: 276–284.
- Lackman, P., et al.** (2011). Jasmonate signaling involves the abscisic acid receptor PYL4 to regulate metabolic reprogramming in *Arabidopsis* and tobacco. *Proc. Natl. Acad. Sci. USA* **108**: 5891–5896.
- Liu, X.C., Yu, C.W., Duan, J., Luo, M., Wang, K.C., Tian, G., Cui, Y.H., and Wu, K.Q.** (2012). HDA6 directly interacts with DNA methyltransferase MET1 and maintains transposable element silencing in *Arabidopsis*. *Plant Physiol.* **158**: 119–129.
- Page, M., Sultana, N., Paszkiewicz, K., Florance, H., and Smirnov, N.** (2012). The influence of ascorbate on anthocyanin accumulation during high light acclimation in *Arabidopsis thaliana*: Further evidence for redox control of anthocyanin synthesis. *Plant Cell Environ.* **35**: 388–404.
- Papadopoulos, J.S., and Agarwala, R.** (2007). COBALT: Constraint-based alignment tool for multiple protein sequences. *Bioinformatics* **23**: 1073–1079.
- Paszowski, J., and Grossniklaus, U.** (2011). Selected aspects of transgenerational epigenetic inheritance and resetting in plants. *Curr. Opin. Plant Biol.* **14**: 195–203.
- Probst, A.V., Fagard, M., Proux, F., Mourrain, P., Boutet, S., Earley, K., Lawrence, R.J., Pikaard, C.S., Murfett, J., Furner, I., Vaucheret, H.,**

- and Mittelsten Scheid, O. (2004). *Arabidopsis* histone deacetylase HDA6 is required for maintenance of transcriptional gene silencing and determines nuclear organization of rDNA repeats. *Plant Cell* **16**: 1021–1034.
- Roguev, A., and Krogan, N.J. (2007). SIN-fully silent: HDAC complexes in fission yeast. *Nat. Struct. Mol. Biol.* **14**: 358–359.
- Rossi, V., Locatelli, S., Varotto, S., Donn, G., Pirona, R., Henderson, D.A., Hartings, H., and Motto, M. (2007). Maize histone deacetylase hda101 is involved in plant development, gene transcription, and sequence-specific modulation of histone modification of genes and repeats. *Plant Cell* **19**: 1145–1162.
- Roudier, F., Teixeira, F.K., and Colot, V. (2009). Chromatin indexing in *Arabidopsis*: An epigenomic tale of tails and more. *Trends Genet.* **25**: 511–517.
- Saleh, A., Alvarez-Venegas, R., Yilmaz, M., Le, O., Hou, G.C., Sadler, M., Al-Abdallat, A., Xia, Y.N., Lu, G.Q., Ladunga, I., and Avramova, Z. (2008). The highly similar *Arabidopsis* homologs of trithorax ATX1 and ATX2 encode proteins with divergent biochemical functions. *Plant Cell* **20**: 568–579.
- Sani, E., Herzyk, P., Perrella, G., Colot, V., and Amtmann, A. (2013). Hyperosmotic priming of *Arabidopsis* seedlings establishes a long-term somatic memory accompanied by specific changes of the epigenome. *Genome Biol.* **14**: R59.
- Shahbazian, M.D., and Grunstein, M. (2007). Functions of site-specific histone acetylation and deacetylation. *Annu. Rev. Biochem.* **76**: 75–100.
- Skirycz, A., et al. (2011). Survival and growth of *Arabidopsis* plants given limited water are not equal. *Nat. Biotechnol.* **29**: 212–214.
- Song, C.P., Agarwal, M., Ohta, M., Guo, Y., Halfter, U., Wang, P.C., and Zhu, J.K. (2005). Role of an *Arabidopsis* AP2/EREBP-type transcriptional repressor in abscisic acid and drought stress responses. *Plant Cell* **17**: 2384–2396.
- Song, C.P., and Galbraith, D.W. (2006). AtSAP18, an orthologue of human SAP18, is involved in the regulation of salt stress and mediates transcriptional repression in *Arabidopsis*. *Plant Mol. Biol.* **60**: 241–257.
- Takezawa, D., Komatsu, K., and Sakata, Y. (2011). ABA in bryophytes: How a universal growth regulator in life became a plant hormone? *J. Plant Res.* **124**: 437–453.
- Tanaka, M., Kikuchi, A., and Kamada, H. (2008). The *Arabidopsis* histone deacetylases HDA6 and HDA19 contribute to the repression of embryonic properties after germination. *Plant Physiol.* **146**: 149–161.
- Tian, L., and Chen, Z.J. (2001). Blocking histone deacetylation in *Arabidopsis* induces pleiotropic effects on plant gene regulation and development. *Proc. Natl. Acad. Sci. USA* **98**: 200–205.
- To, T.K., et al. (2011). *Arabidopsis* HDA6 regulates locus-directed heterochromatin silencing in cooperation with MET1. *PLoS Genet.* **7**: e1002055.
- Voinnet, O., Rivas, S., Mestre, P., and Baulcombe, D. (2003). An enhanced transient expression system in plants based on suppression of gene silencing by the p19 protein of tomato bushy stunt virus. *Plant J.* **33**: 949–956.
- Wang, B., Davenport, R.J., Volkov, V., and Amtmann, A. (2006). Low unidirectional sodium influx into root cells restricts net sodium accumulation in *Thellungiella halophila*, a salt-tolerant relative of *Arabidopsis thaliana*. *J. Exp. Bot.* **57**: 1161–1170.
- Winter, D., Vinegar, B., Nahal, H., Ammar, R., Wilson, G.V., and Provart, N.J. (2007). An “Electronic Fluorescent Pictograph” browser for exploring and analyzing large-scale biological data sets. *PLoS ONE* **2**: e718.
- Xu, C.R., Liu, C., Wang, Y.L., Li, L.C., Chen, W.Q., Xu, Z.H., and Bai, S.N. (2005). Histone acetylation affects expression of cellular patterning genes in the *Arabidopsis* root epidermis. *Proc. Natl. Acad. Sci. USA* **102**: 14469–14474.
- Yamaguchi-Shinozaki, K., and Shinozaki, K. (2006). Transcriptional regulatory networks in cellular responses and tolerance to dehydration and cold stresses. *Annu. Rev. Plant Biol.* **57**: 781–803.
- Yang, X.J., and Seto, E. (2008). The Rpd3/Hda1 family of lysine deacetylases: From bacteria and yeast to mice and men. *Nat. Rev. Mol. Cell Biol.* **9**: 206–218.
- Yu, C.W., Liu, X.C., Luo, M., Chen, C.Y., Lin, X.D., Tian, G., Lu, Q., Cui, Y.H., and Wu, K.Q. (2011). HISTONE DEACETYLASE6 interacts with FLOWERING LOCUS D and regulates flowering in *Arabidopsis*. *Plant Physiol.* **156**: 173–184.
- Zhou, C.H., Zhang, L., Duan, J., Miki, B., and Wu, K.Q. (2005). HISTONE DEACETYLASE19 is involved in jasmonic acid and ethylene signaling of pathogen response in *Arabidopsis*. *Plant Cell* **17**: 1196–1204.
- Zhou, J.L., Wang, X.F., He, K., Charron, J.B.F., Elling, A.A., and Deng, X.W. (2010). Genome-wide profiling of histone H3 lysine 9 acetylation and dimethylation in *Arabidopsis* reveals correlation between multiple histone marks and gene expression. *Plant Mol. Biol.* **72**: 585–595.
- Zhu, J., Jeong, J.C., Zhu, Y., Sokolchik, I., Miyazaki, S., Zhu, J.K., Hasegawa, P.M., Bohnert, H.J., Shi, H., Yun, D.J., and Bressan, R.A. (2008). Involvement of *Arabidopsis* HOS15 in histone deacetylation and cold tolerance. *Proc. Natl. Acad. Sci. USA* **105**: 4945–4950.
- Zhu, Z.Q., et al. (2011). Derepression of ethylene-stabilized transcription factors (EIN3/EIL1) mediates jasmonate and ethylene signaling synergy in *Arabidopsis*. *Proc. Natl. Acad. Sci. USA* **108**: 12539–12544.